# FLUORESCENCE DEPOLARIZATION MEASUREMENTS ON ORIENTED MEMBRANES

MARC ADLER AND THOMAS R. TRITTON
*Department of Chemistry, Cornell University, Ithaca, New York 14853 and Department of Pharmacology, University of Vermont School of Medicine, Burlington, Vermont 05405*

ABSTRACT  We describe the theory and experimental application of fluorescence depolarization measurements on small molecules bound to oriented phospholipid bilayers. The results yield insight into both the orientation and the rotational motion of fluorophores in a membrane environment. To accomplish this the angular distribution of polarized fluorescence intensities is measured on a membrane preparation consisting of stacked phospholipid bilayers oriented in a known coordinate system. Considerably more information is available from this data than in comparable solution phase measurements. Three parameters are derived from the data: the rate of rotational diffusion and the second and fourth degree order parameters. These latter two parameters provide an assessment of the average distribution of fluorophore orientation in the membrane bilayer. The data have been carefully examined for systematic experimental artifacts and new protocols are presented which help to eliminate errors that have not been amply treated in the past. We present data for two types of fluorescent molecules: (*a*) conventional membrane probes like diphenylhexatriene, perylene and anthroyloxy fatty acids; and (*b*) the anticancer agent adriamycin and several congeneric anthracycline antibiotics. The results show that the hydrocarbon core of membranes is more rigid than previously thought, particularly above the thermal phase transition temperature. We also show that the orientation of small molecules is sensitive to both the phospholipid composition and to the interaction of specific functional groups with the lipid bilayer. The results are discussed in terms of energetic models describing the general patterns for the binding of small molecules to biological membranes.

## INTRODUCTION

Many investigators have used fluorescence spectroscopy to study the dynamics of membranes. Measurements are generally performed by adding a fluorescent probe to the experimental sample. The probe binds to the lipid bilayer, thereby limiting its rotational freedom. The degree of this constraint is assayed by the depolarization of the exciting light caused by the probe's motion. Generally, the measurements are performed on isotropic solution samples, both to simplify the experimental protocols and to reduce artifacts that stem from reflection and light scattering.

One of the drawbacks of this methodology is the lack of a theoretical framework which relates the observed experimental quantities to a detailed description of the probe's motions. Fluorescent molecules have a relatively short relaxation time compared with corresponding probes used in ESR (nitroxide spin probes) and nuclear magnetic resonance (e.g., deuterium labeled lipids). Thus one cannot assume that motion is fast compared with the fluorescence lifetime of the probe. Initially, investigators assumed that the probe underwent hindered isotropic rotation. Using fluorescence depolarization values and lifetimes, one derives rotational rates which reflect the microviscosity of the probes environment (Perrin, 1936). More recent work which employs time resolved fluorescence measurements provides more information on the probe's movement (Kawato et al., 1977; Lakowicz et al., 1979, 1980; Stubbs et al., 1981; Kinosita and Ikegami, 1984). These results conclusively show that most probe molecules undergo anisotropic rotations, clearly demonstrating the need for a more sophisticated theoretical framework.

Working towards this goal several laboratories have performed fluorescence measurements on globally oriented samples (Yguerabide and Stryer, 1971; Badley et al., 1971, 1973, 1976; Frehland et al., 1982; Kooyman et al., 1981, 1983; Vos et al., 1983). The data are acquired in anisotropic fashion, that is the orientation of the lipid bilayer in the laboratory frame is known. Therefore, the data reflects the anisotropy of the membranes and shows an increased sensitivity to the orientation of the probe.

There are several drawbacks to this approach. Unlike solution phase studies, the experimental samples are planar and they are large compared with the wavelength of visible light. This results in very complex patterns of refraction and reflection. Comprehensive controls must be developed in order to eliminate experimental artifacts. Another consideration is that previous measurements were performed on custom built fluorescence spectrophotometers. The high cost associated with the construction of this equipment has limited the application of the technique.

This paper describes a new experimental procedure for

fluorescence measurements on globally oriented membranes. The internal controls are more extensive than in any of the previous protocols. We have carefully examined our data for the presence of artifacts. After several modifications, the artifacts were reduced below the level of detection. Furthermore, the requirements for customized apparatus were reduced to only a simple sample holder. Experimental results from several membrane probes as well as fluorescent anticancer drugs are presented below.

## MATERIALS AND METHODS

### Materials

Lipids were purchased from Sigma Chemical Co., St. Louis, MO and were used without further purification. Purity was monitored by TLC analysis and the lipids were found to be at least 98% pure before and after sonication. The sources of the various fluorescence probes are enumerated in Table I. The black glass slides were purchased from A&W Stained Glass, New Haven, CT. This material has no detectable fluorescence at any of the wavelengths used in the experiments. The water was double distilled to insure the proper formation of the oriented membranes. All glassware was washed in a concentrated sulfuric and chromic acid solution, followed by copious rinses with water.

### Experimental Technique

*Preparation of Samples.* Macroscopically oriented membranes were prepared by the following protocol. The probe molecule and lipid(s) were dissolved in methanol. The probe was added in 1/400 molar ratio with the lipid and the methanol removed by evaporation under $N_2$ at 45°. The mixture was then resuspended in water by vortexing at a lipid concentration of 22 mg/ml. This solution was sonicated using a bath type sonicator (Laboratory Supply Corp., Hicksville, NY) for 1 to 3 h until the solution became optically clear.

In the next step ~150 ul of the lipid solution was placed on the clean surface of a black piece of glass. Since the formation of the oriented membranes resembles a crystallization, precautions must be taken to insure the glass is scrupulously clean and the solutions free from contaminants. The excess water was removed by evaporation at 86% humidity.

To insure the full hydration of the sample, a drop of water was placed on top of the dried membranes about 1 h before use. Immediately before the experiment the excess water was removed by a stream of $N_2$. Small imperfections in the edges of the membrane were removed with a razor blade.

The following techniques were used to test the smoothness and orientation of the membranes. Sample membranes were prepared on clear microscope slides. When placed between two crossed polarizers, the membranes appeared completely black, thus indicating that the membranes were highly oriented. The smoothness of the membranes was assayed by reflecting the output of an argon ion laser off the front surface. By studying the angle of reflection the variations in the flatness of the membrane could be determined. The front surface was found to be level to within ¼ of a degree.

*Collection of Data.* Experiments were performed on a SLM 4800 fluorescence spectrophotometer with modified sample compartment. The cuvette holder was removed and replaced with a custom built sample holder (Fig. 1). A diagram of the equipment appears in Fig. 2. When necessary, the sample was heated (or cooled) by water circulating through a flow chamber. The black glass slide forms one wall of the chamber. The chamber was mounted directly onto the $Y'$ translator (Ty) of the sample holder. Temperature was monitored by a flat surface thermistor.

Table I summarizes the various combinations of filters and slit widths used for different probes. In most cases the excitation wavelength was selected by a diffraction grating monochromator with a band pass of 4 nm. Short pass filters (Melles Griot; Zevenaar, Netherlands) were used for the anthracycline antibiotics to remove overtones of the exciting beam. The emitted light passed through long pass filters (Schott, Germany). The cutoff wavelength was at least 50 nm > the excitation wavelength. Since the intensity of scattered light is appreciably greater than the corresponding solution measurements, the optical filters were used in pairs.

During the mathematical analysis, it was assumed that the light comes from a point source. Iris diaphragms (Melles Griot; Zevenaar, Netherlands) were used to narrow the light path. The apertures were set to 9 mm, which corresponds to a 10° arc of light. Narrower settings gave identical results.

The coordinates of the excitation and observation vectors must be determined relative to the membrane coordinate system. Throughout this paper the vector e is the electric vector of the excitation beam, o is the electric vector of the observed florescence and $\theta$, the observation angle, is the angle between the $Y$ and $Y'$ axis (see Fig. 3). An e or an o with the subscript V (vertical) denotes light polarized in the plane of the membrane and parallel to the $X'$ axis. The membrane coordinates of these vectors are (1, 0, 0). Similarly, an e or an o with the subscript H (horizontal) denotes light polarized perpendicular to the $X'$ axis and aligned with the $Y'$ axis for the excitation beam or $Z'$ for the observed

TABLE I
OPTICAL INFORMATION

| Compound | Abbreviation | Excitation wavelength | Long pass filter | Short pass filter | Band pass width | Source |
|---|---|---|---|---|---|---|
| | | | nm | nm | nm | |
| 12-9-anthroyl stearic acid | 12-AS | 385 or 347 | 1 × 470 | None | 4 | Molecular probes |
| N,N'-di(octadecyl) oxa-carbocyanine | CY | 493 | 1 × 550 | None | 4 | Molecular probes |
| Perylene | PER | 441 or 394 | 1 × 500 | None | 4 | Aldrich |
| Quinizarin | QUN | 470 | 2 × 550 | 2 × 500 | 4 | Aldrich |
| Diphenylhexatriene | DPH | 360 | 2 × 418 | None | 1 | Aldrich |
| Anthracycline antibiotics | As noted* | 470 | 2 × 550[‡] | 2 × 500[‡] | 4 | As noted* |

*Sources and abbreviation for the anthracycline antibiotics are as follows: adriamycin (adr), daunomycin (dau), 4-methoxydaunomycin (met-dau), N,N-dimethyaminoadriamycin (N,N-adr), N,N-dimethyaminodaunomycin (N,N-dau), 4'-epiadriamycin (epi-adr), were a gift of Dr. Lenonard Kedda of the Division of Cancer Treatment, National Cancer Institute. Adriamycin aglycone (adr-ag) and daunomycin aglycone (dau-ag) were a gift of Dr. Thomas Burke, City of Hope. Carminomycin (car) was provided by Bristol Laboratories, Syracuse, NY.
[‡]Only one long pass filter and one short pass filter was used for N,N'-dimethyaminodaunomycin.
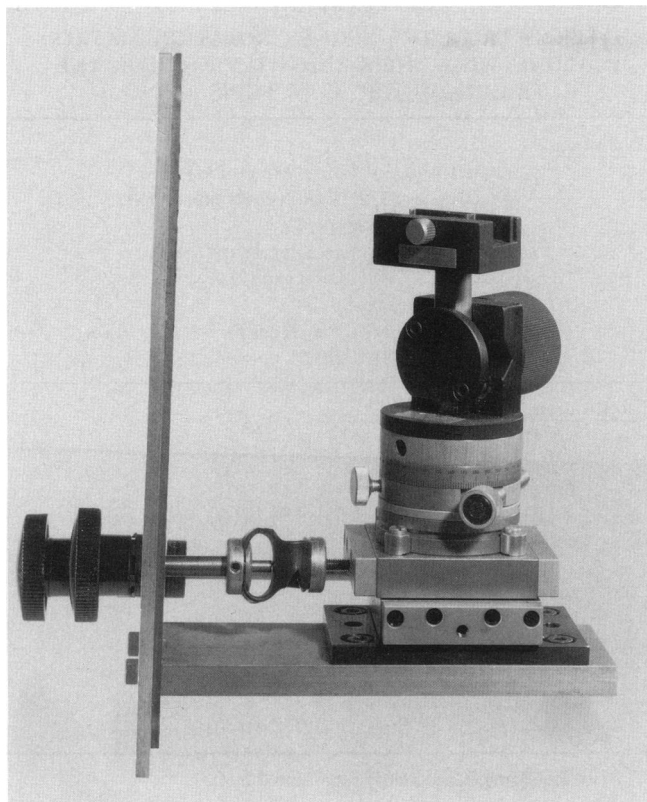
FIGURE 1 The Sample Holder. The components are as follows; (S) side plate, (Ty) and (Tz) the Y' and Z' translators, (Ey) and (Ez) external controls for the translator, (Rx) the X' rotator and (P) the plate holder. The holder is mounted on a side plate which is cut to the same dimensions as the side plate of the sample chamber in the SLM 4800 fluorometer. It blots directly onto the fluorometer. The individual components of the sample holder were purchased from Klinger Scientific Corp., Richmond Hill, NY, Winfred M. Berg Inc., East Rockaway, NY, or they were manufactured on the premises.

fluorescence. In the absence of refraction, the membrane coordinates of these vectors are $(0, \cos \theta, \sin \theta)$ and $(0, \sin \theta, \cos \theta)$ respectively.

Fluorescence intensities are measured for different settings of the angle $\theta$, which is varied by rotating the sample around the $X'$ axis (Fig. 2 and 3). At each angle, four intensities are measured: $Ie_V o_V$, $Ie_H o_H$, $Ie_V o_H$, and
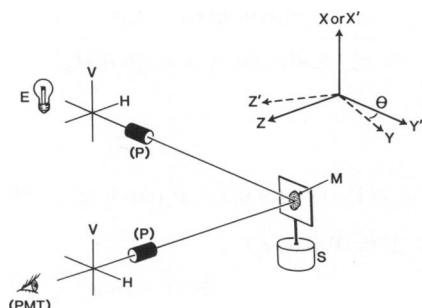


FIGURE 2 Equipment Configuration. The symbols are as follows: (E) 500 watt Xenon arc excitation lamp, (PMT) photomultiplier tube and observation optics, (P) Glan-Thompson polarizers, (S) sample holder, (B) black glass slide and (M) oriented membrane. The laboratory $(X', Y', Z')$ and membrane $(X, Y, Z)$ coordinae system have been included for reference. The angle between the $Y$ and $Y'$ axes is $\theta$.
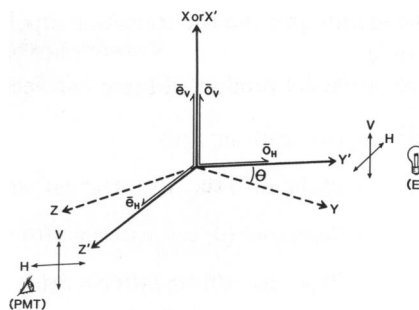


FIGURE 3 Coordinate Systems in the Laboratory and Membrane Frames of Reference. The $(X, Y, Z)$ coordinates system refers to the membrane and the $(X', Y', Z')$ coordinates refer to the laboratory. The $Z$ axis is the normal of the membrane. In the laboratory frame of reference, the $X'$ axis is the vertical and is parallel to the $X$ axis of the membrane. The four vectors $e_H$, $e_V$, $o_H$ and $o_V$ have been included for reference.

$Ie_H o_H$. A typical data set consists of the four intensities measured at 12 different angles for a total of 48 data points. The experimental measurements are then fitted to theoretical equations for the distribution of polarized light (see mathematical analysis).

The experimental sample was aligned using the following protocol. The excitation and observation polarizers were set to vertical and horizontal respectively ($Ie_V o_H$). The sample holder was then moved back and forth in the horizontal ($Y'$, $Z'$) plane until the maximum signal intensity was obtained. Experiments show that the precision of the data is greatly affected by the alignment.

The experimental intensities must be corrected for polarization of the exciting light by the monochromator grating. This stems from differential transmission of the parallel and perpendicular components of the excitation beam. The relative intensity of the two components is determined from the ratio of $Ie_H e_V$ to $Ie_V o_H$. The angular distribution of this ratio is given by:

$$\frac{Ie_H o_V}{Ie_V o_H} = F \frac{A \sin^2 \theta + 1}{A \cos^2 \theta + 1}. \tag{1}$$

$A$ is a constant determined by nonlinear regression and $F$ is the ratio of the horizontal and vertical components of the light.

## MATHEMATICAL ANALYSIS

In the absence of random experimental errors, the experimental data can be simulated with three independent parameters. Each parameter reflects the chromophore's rotational rate and its average orientation. Equations must be developed that relate the laboratory measurements to the probe's motion.

The interaction of light with a chromophore is a dipole–dipole interaction. Therefore, it is also proportional to the square of the dot product of the two vectors. The coordinates of the excitation vector, $\mathbf{e}$, are defined as:

$$\mathbf{e} = (e_x, e_y, e_z) \tag{2}$$

The $Z$ axis ($e_z$) is the normal of the membrane. The coordinates of the absorption dipole, represented by the vector of the chromophore $\mathbf{c}(t)$ at $t = 0$, are: $\mathbf{c}(0) = [\cos \alpha(0) \sin \beta(0), \sin \alpha(0) \sin \beta(0), \cos \beta(0)]$ The coordinates are given in terms of the spherical coordinates, $\alpha$ and $\beta$. $\beta$ is the polar angle, i.e., the angle between the

normal of the membrane and the transition dipole. $\alpha$ is the azimuthal angle.

The square of the dot product of these two vectors is:

$$|e \cdot c(0)|^2 = e_x^2 \cos^2 \alpha(0) \sin^2 \beta(0)$$

$$+ e_y^2 \sin^2 \alpha(0) \sin^2 \beta(0) + e_z^2 \cos^2 \beta(0)$$

$$+ 2e_x e_y \sin \alpha(0) \cos \alpha(0) \sin^2 \beta(0)$$

$$+ 2e_x e_z \cos \alpha(0) \sin \beta(0) \cos \beta(0)$$

$$+ 2e_y e_z \sin \alpha(0) \sin \beta(0) \cos \beta(0). \quad (3)$$

Similar results are derived for the square of the dot product of the observation vector, $o$, and the emission dipole, $c(t)$, using the following coordinates:

$$o = (o_x, o_y, o_z)$$

$$c(t) = (\cos \alpha[t] \sin \beta[t], \sin \alpha [t]$$

$$\cdot \sin \beta[t], \cos \beta[t]). \quad (4 \text{ and } 5)$$

The observed fluorescence intensities are proportional to the product of the two squares. The resulting equation has 36 terms, but fortunately the complexity of the calculation can be greatly reduced. The first simplification stems from the uniaxial symmetry of biological membranes. The angle $\alpha$ is averaged over 360° and any terms with odd factors of $\cos \alpha$ and $\sin \alpha$ are equal to zero.

To further simplify the mathematics, terms from the Wigner rotation matrix are substituted for the trigonometric functions of $\alpha$ and $\beta$. This technique, originally developed for quantum mechanics (Wigner, 1959), has been applied to problems in membrane biochemistry (Zannoni et al., 1983; Szabo, 1980, 1984). The necessary substitutions, as well as the definitions of the terms, appear in Table II.

The uniaxial symmetry of the membranes is reflected in the following equations:

$$\langle D_{mo}^2[\Omega(0)] \rangle = \delta_{mo} \langle P_2 \rangle P_2(\cos u_a) \quad (6)$$

$$\langle D_{mo}^2[\Omega(t)] \rangle = \delta_{mo} \langle P_2 \rangle P_2(\cos u_e) \quad (7)$$

$$\langle D_{mo}^2[\Omega(0)] D_{mo}^{2*}[\Omega(t)] \rangle = \delta_{mn} H_m(t) \quad (8)$$

$$D_{mo}^2[\Omega(t)] = (-1)^m D_{mo}^{2*}[\Omega(t)] \quad (9)$$

$\delta_{mn}$ is the Kronecker-delta function. $\langle P_2 \rangle$ is the second degree order parameter. It is equivalent to the time averaged value of the second degree Legendre polynomial[1] of $\cos \beta$ and it measures the average orientation of the probe. The symbol S is commonly substituted for $\langle P_2 \rangle$ in the literature. The angles $u_a$ and $u_e$ are the angles between the absorption and emission dipoles and the central axis of the probe. The term $H_m(t)$ is the $m^{th}$ degree correlation coefficient. These are defined in Eq. 8 and can be approxi-

---

[1]The $n^{th}$ Legendre polynomial of $x$ is denoted by $P_n(x)$. For $n = 2$: $P_2(x) = \frac{1}{2}(3x^2 - 1)$.

## TABLE II
### TERMS FROM THE WIGNER ROTATION MATRIX ALONG WITH THEIR SUBSTITUTIONS FOR THE TRIGONOMETRIC FUNCTIONS $\alpha$ AND $\beta$

Definitions

$$D_{20}^2(\Omega) = (3/8)^{1/2} \sin^2 \beta \exp(-2i\alpha)$$
$$D_{10}^2(\Omega) = -(3/2)^{1/2} \sin \beta \cos \beta \exp(-i\alpha)$$
$$D_{00}^2(\Omega) = \frac{1}{2}(3 \cos^2 \beta - 1)$$
$$D_{-10}^2(\Omega) = (3/2)^{1/2} \sin \beta \cos \beta \exp(i\alpha)$$
$$D_{-20}^2(\Omega) = (3/8)^{1/2} \sin^2 \beta \exp(2i\alpha)$$
$$d_{00}^2(\beta) = \frac{1}{2}(3 \cos^2 \beta - 1)$$
$$d_{\pm 10}^2(\beta) = \mp (3/2)^{1/2} \sin \beta \cos \beta$$
$$d_{\pm 20}^2(\beta) = (3/8)^{1/2} \sin^2 \beta$$

Substitutions

$$\cos^2 \beta(t) = \frac{1}{3}\{1 + 2 D_{00}^2[\Omega(t)]\}$$

$$\sin^2 \beta(t) \sin^2 \alpha(t) = \frac{1}{3}\{1 - D_{00}^2[\Omega(t)] - (3/2)^{1/2}(D_{20}^2[\Omega(t)] + D_{-20}^2[\Omega(t)]\}$$

$$\cos^2 \alpha(t) \sin^2 \beta(t) = \frac{1}{3}[1 - D_{00}^2[\Omega(t)] - (3/2)^{1/2}\{D_{20}^2[\Omega(t)] + D_{-20}^2[\Omega(t)]\}]$$

$$\sin \alpha(t) \cos \alpha(t) \sin^2 \beta(t) = \frac{1}{3}\{-i(3/2)^{1/2}[D_{20}^2[\Omega(t)] + D_{-20}^2\{\Omega(t)\}]\}$$

$$\sin \alpha(t) \sin \beta(t) \cos \beta(t) = \frac{1}{3}\{i(3/2)^{1/2}[D_{10}^2\{\Omega(t)\} + D_{-10}^2\{\Omega(t)\}]\}$$

$$\cos \alpha(t) \cos \beta(t) \sin \beta(t) = \frac{1}{3}\{-(3/2)^{1/2}[D_{10}^2(\Omega(t)) + D_{-10}^2(\Omega(t))]\}$$

The two Euler angles are jointly represented by $\Omega$.

mated by single exponential (Eqs. 37 and 38). $\langle P_2 \rangle$ measures the static distribution of the probe. The correlation coefficients reflect the rate of the rotation.

Making the appropriate substitutions, and gathering all the like terms, the observed intensity, $I$, is:

$$I = e_z^2 o_z^2 I_{zz}$$

$$+ (e_z^2 o_x^2 + e_z^2 o_y^2) I_{zx}$$

$$+ (e_x^2 o_z^2 + e_y^2 o_z^2) I_{xz}$$

$$+ (e_x^2 o_x^2 + e_y^2 o_y^2) I_{xx}$$

$$+ (e_x^2 o_y^2 + e_y^2 o_x^2) I_{xy}$$

$$+ 2e_x e_y o_x o_y (I_{xx} - I_{xy})$$

$$+ 4(e_x e_z o_x o_z + e_y e_z o_y o_z) I_{oa}, \quad (10)$$

where:

$$I_{zz} = \frac{1}{9}\{1 + 2\langle P_2 \rangle [P_2(\cos u_a) + P_2(\cos u_e)] + 4H_0(t)\} \quad (11)$$

$$I_{zx} = \frac{1}{9}[1 + 2\langle P_2 \rangle P_2(\cos u_a)$$
$$- \langle P_2 \rangle P_2(\cos u_e) - 2H_0(t)] \quad (12)$$

$$I_{xz} = \frac{1}{9}[1 + 2\langle P_2 \rangle P_2(\cos u_e)$$
$$- \langle P_2 \rangle P_2(\cos u_a) - 2H_0(t)] \quad (13)$$

$$I_{xy} = \frac{1}{9}\{1 - \langle P_2 \rangle [P_2(\cos u_a)$$
$$+ P_2(\cos u_e)] + H_0(t) - 3H_2(t)\} \quad (14)$$

$$I_{xx} = \tfrac{1}{9}\{1 - \langle P_2 \rangle \, [P_2(\cos \mathbf{u}_a)$$

$$+ \, P_2(\cos \mathbf{u}_e)] + H_0(t) + 3H_2(t)\} \quad (15)$$

$$I_{oa} = \tfrac{4}{3}H_1(t) \quad (16)$$

$$(I_{xx} - I_{xy}) = \tfrac{2}{3}H_2(t) \quad (17)$$

The factors $I_{ij}$ represent the six independent fluorescent intensities. Any intensity measured in the laboratory is represented by a linear combination of these intensities. The subscripts $i$ and $j$ refer to the Cartesian coordinate system. The intensity $I_{zx}$ is measured by aligning the excitation dipole with the $Z$ axis and the observation dipole with the $X$ axis. The intensity $I_{oa}$ cannot be measured directly and represents the "off axis" component of the fluorescence.

In order to simulate the experimental intensities the following unit vectors are substituted into Eq. 10:

$$\mathbf{e}_V = (1, 0, 0) \quad (18)$$

$$\mathbf{e}_H = \{0, [1 - \sin^2 (\theta)/n^2]^{1/2}, \sin (\theta)/n\} \quad (19)$$

$$\mathbf{o}_V = (1, 0, 0) \quad (20)$$

$$\mathbf{o}_H = \{0, [1 - \cos^2 (\theta)/n^2]^{1/2}, \cos (\theta)/n\} \quad (21)$$

The angle $\theta$ is the angle between the observation optics and the plane of the membrane (Figs. 2 and 3). The constant $n$ is the ratio of the refractive index of the sample to that of the surrounding medium. The vectors have been corrected for the refraction of light at the interface of the membrane (Eq. 40). The final expressions for the experimental intensities are:

$$I\mathbf{e}_V\mathbf{o}_V = I_{xx} \quad (22)$$

$$I\mathbf{e}_V\mathbf{o}_H = 1/n^2(I_{xz} - I_{xy}) \cos^2 \theta + I_{xy} \quad (23)$$

$$I\mathbf{e}_H\mathbf{o}_V = F[1/n^2(I_{zx} - I_{xy}) \sin^2 \theta + I_{xy}] \quad (24)$$

$$\begin{aligned} I\mathbf{e}_H\mathbf{o}_H = &\, F/n^4(I_{xx} + I_{zz} - I_{xz} - I_{zx}) \sin^2 \theta \cos^2 \theta \\ &+ F/n^2(I_{xz} - I_{zx}) \cos^2 \theta \\ &+ F/n^2[I_{zx} + (n^2 - 1)I_{xx}] \\ &- F/n^4 I_{oa}[\sin^2 \theta \cos^2 \theta (n^2 - \sin^2 \theta)(n^2 - \cos^2 \theta)]^{1/2}. \end{aligned}$$

$$(25)$$

The factor $F$ has been included to correct for the polarization of the exciting light caused by the diffraction grating. It equals the relative intensity of $e_H/e_V$.

These equations are equivalent to those derived independently by Van derMeer et al. (1982). However, the nomenclature is changed for reasons of clarity.

Further simplification is achieved by assuming the transition dipoles are parallel to the central axis of the fluorophore. This implies that $P_2(\cos \mathbf{u}_a)$ and $P_2(\cos \mathbf{u}_e)$ are equal to 1. Experimental justification for this assemption is presented in the result section. The six independent intensi-

ties become:

$$I_{zz} = \tfrac{1}{9}[1 + 4\langle P_2 \rangle + 4H_0(t)] \quad (26)$$

$$I_{zx} = I_{xz} = \tfrac{1}{9}[1 + \langle P_2 \rangle - 2H_0(t)] \quad (27)$$

$$I_{xy} = \tfrac{1}{9}[1 - 2\langle P_2 \rangle + H_0(t) - 3H_2(t)] \quad (28)$$

$$I_{xx} = \tfrac{1}{9}[1 - 2\langle P_2 \rangle + H_0(t) + 3H_2(t)] \quad (29)$$

$$I_{oa} = \tfrac{4}{3}H_1(t). \quad (30)$$

The approximate values for the correlation coefficients, $H_m(t)$, are derived by Szabo (1984). These approximations relate $H_m(t)$ to the values of the second and fourth degree order parameters, $\langle P_2 \rangle$ and $\langle P_4 \rangle$ respectively, and the rate of rotation. $\langle P_2 \rangle$ and $\langle P_4 \rangle$ are defined as follows:

$$\langle P_2 \rangle = \langle \tfrac{1}{2}(3 \cos^2 \beta - 1) \rangle \quad (31)$$

$$\langle P_4 \rangle = \langle \tfrac{1}{8}(35 \cos^4 \beta - 30 \cos^2 \beta + 3) \rangle. \quad (32)$$

These are the time average values for the second and fourth degree Legendre polynomials of cos $\beta$. The equations can be restated as

$$\langle P_N \rangle = \int_0^{\pi/2} P(\beta) P_N(\cos \beta) \sin \beta \, d\beta \quad (33)$$

$\langle P_N \rangle$ is the $N^{th}$ degree Legendre polynomial. $P(\beta)$ is the angular distribution function. It measures the relative probability of finding a probe tilted at the angle $\beta$. $\langle P_2 \rangle$ and $\langle P_4 \rangle$ reflect the average orientation of the probe. They are derived independently from any model for the motion of the probe. Therefore, the data analysis is not biased by any inaccuracies of the modeling assumptions. In theory, the results will be consistent with the data obtained from any subsequent experiments that yield more information on the dynamics of membrane probes.

A plot of $\langle P_2 \rangle$ and $\langle P_4 \rangle$ verses the polar angle $\beta$ appears in Fig. 4.

Qualitatively the second degree order parameter, $\langle P_2 \rangle$, is a measure of the average tilt of the probe. If the probe is closely aligned with the normal of the membrane, then $\langle P_2 \rangle$ is positive. A negative value for $\langle P_2 \rangle$ means that the
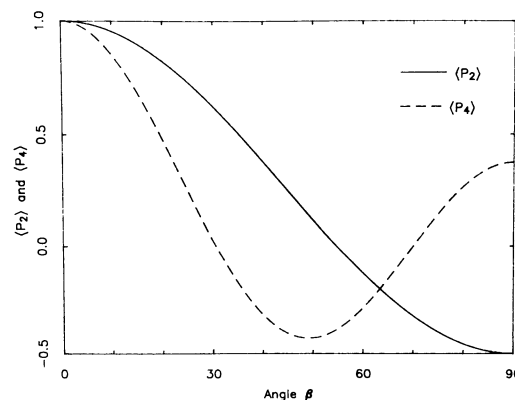


FIGURE 4   Plots of $\langle P_2 \rangle$ and $\langle P_4 \rangle$ versus $\beta$.

probe is aligned parallel to the plane of the membrane. The values for $\langle P_2 \rangle$ vary monotomically from 1 to −0.5. A totally random or disoriented probe would have a $\langle P_2 \rangle$ value of 0. Without more information, this can not be distinguished from a probe aligned at the magic angle, 54.7°.

Interpretation of the fourth degree order parameter, $\langle P_4 \rangle$, is more complex. Like $\langle P_2 \rangle$, a totally ordered probe yields a $\langle P_4 \rangle$ value of 1 and for a disordered probe, $\langle P_4 \rangle$ = 0. However, there is no simple interpretation for intermediate values. Qualitatively, it modifies the width of the distribution. As $\langle P_4 \rangle$ increases, the distribution becomes narrower. However, the extent of the narrowing is a function of both $\langle P_2 \rangle$ and $\langle P_4 \rangle$.

The order parameters themselves are part of an infinite series. If all the terms are known then $P(\beta)$ is calculated from the equation.

$$P(\beta) = \sum_N \frac{2N + 1}{2} \langle P_N \rangle P_N(\cos \beta) \qquad N \text{ is even} \quad (34)$$

Unfortunately this series converges rather slowly. The equation yields negative values for $P(\beta)$ if it is truncated after two terms. Therefore, an alternate equation is required in order to approximate $P(\beta)$ from $\langle P_2 \rangle$ and $\langle P_4 \rangle$. The equation is equivalent to a model for the orientation and motion of the probe. To some extent the final choice of the model is somewhat arbitrary. Since the higher order parameters are not known, many functions will be consistent with the data. For various reasons discussed below the following model was selected:

$$P(\beta) = \exp\left(-U(\beta)/kT\right)\bigg/ \int_0^{\pi/2}$$

$$\cdot \exp[-U(\beta)/kT] \sin \beta \, d\beta, \quad (35)$$

where $U(\beta)$ is the effective energy potential for the angle $\beta$. This potential is defined by the equation:

$$U(\beta) = k|\sin \beta| P \text{ for } \langle P_2 \rangle > 0$$

$$= k|\cos \beta| P \text{ for } \langle P_2 \rangle < 0 \quad (36)$$

The model for the distribution function is referred to as the power model. It has a single maximum that is centered on either the membrane normal, for positive $\langle P_2 \rangle$, or the plane of the bilayer, for negative $\langle P_2 \rangle$. The factor $k$ is the maximum energy difference between the most and least favorable orientations. The term $p$ describes how rapidly the free energy increases as the probe tilts away from its preferred orientation. Generally the small values of $p$ imply a narrow distribution near the maximum. As a point of reference, several calculated angular distributions appear in Fig. 5.

The approximate values of the correlation coefficients,



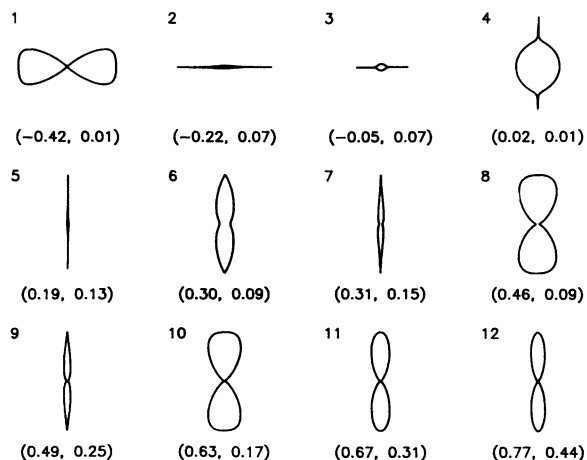| 1 | 2 | 3 | 4 |
| (−0.42, 0.01) | (−0.22, 0.07) | (−0.05, 0.07) | (0.02, 0.01) |
| 5 | 6 | 7 | 8 |
| (0.19, 0.13) | (0.30, 0.09) | (0.31, 0.15) | (0.46, 0.09) |
| 9 | 10 | 11 | 12 |
| (0.49, 0.25) | (0.63, 0.17) | (0.67, 0.31) | (0.77, 0.44) |

FIGURE 5 Plots of the Angular Distribution. The angular distribution for selected probes as defined by the power model. The numbers in parentheses correspond to the values of $\langle P_2 \rangle$ and $\langle P_4 \rangle$ respectively. The plots have been rescaled so that the maximum value of the distribution is the same for each. The probes are

| No. | Probe | Lipid | Temperature |
|-----|-------|-------|-------------|
| 1 | CY | DPPC | 25° |
| 2 | 12-AS | DPPC | 25° |
| 3 | 12-AS | E.L. | 25° |
| 4 | ADR | DPPC | 25° |
| 5 | QUN | DPPC | 25° |
| 6 | MET-DAU | DPPC | 25° |
| 7 | N,N-DAU | DPPC | 25° |
| 8 | ADR | DMPC | 18° |
| 9 | PER | DPPC | 25° |
| 10 | DPH | DMPC | 17° |
| 11 | DPH | DPPC | 25° |
| 12 | DPH | DMPC | 27° |

$H_m(\tau)$ are (Szabo, 1984):

$$H_m(\tau) = \frac{1}{\tau} \int_0^\infty e^{(-t/\tau)} H_m(t) dt$$

$$H_o(\tau) = \langle P_2 \rangle + \{\langle [d_{oo}^2(\beta)]^2 \rangle - \langle P_2 \rangle\}/$$

$$\{1 + u_{oo} D\tau/[\langle (d_{oo}^2(\beta))^2 \rangle - \langle P_2 \rangle]\} \quad (37)$$

For $m \neq o$

$$H_m(\tau) = \langle (d_{mo}^2[\beta])^2 \rangle/(1 + u_{mo} D\tau/\langle [d_{mo}^2\{\beta\}]^2 \rangle). \quad (38)$$

$D$ is the rate of rotational diffusion and $\tau$ is the fluorescence lifetime. The terms $\langle (d_{mo}^2[\beta])^2 \rangle$ and $u_{mo}$ are functions of $\langle P_2 \rangle$ and $\langle P_4 \rangle$ (Table III).

The experimental intensities are predicted by combining the results of Eqs. (22–30; 37, 38). First the intensities are corrected for the reflection and refraction of light at the interface between the lipid and surrounding medium using Fresnel's and Snell's laws respectively (Eqs. 40–42). The intensities must then be normalized to eliminate fluctuations due to sample thickness, optical efficiency, etc. This is done by dividing each of the four intensities measured per

TABLE III

**TABLE III**

$\langle d^2_{mo}(\beta)^2 \rangle$ AND $u_{mo}$ IN TERMS OF $\langle P_2 \rangle$ AND $\langle P_4 \rangle$

$$\langle [d^2_{00}(\beta)]^2 \rangle = \tfrac{1}{5} + \tfrac{2}{7} \langle P_2 \rangle + \tfrac{18}{35} \langle P_4 \rangle$$
$$\langle [d^2_{10}(\beta)]^2 \rangle = \tfrac{1}{5} + \tfrac{1}{7} \langle P_2 \rangle - \tfrac{12}{35} \langle P_4 \rangle$$
$$\langle [d^2_{20}(\beta)]^2 \rangle = \tfrac{1}{5} - \tfrac{2}{7} \langle P_2 \rangle + \tfrac{3}{35} \langle P_4 \rangle$$

and

$$u_{00} = \tfrac{6}{5} + \tfrac{9}{7} \langle P_2 \rangle + \tfrac{72}{35} \langle P_4 \rangle$$
$$u_{10} = \tfrac{6}{5} + \tfrac{3}{7} \langle P_2 \rangle - \tfrac{48}{35} \langle P_4 \rangle$$
$$u_{20} = \tfrac{6}{5} + \tfrac{9}{7} \langle P_2 \rangle + \tfrac{12}{35} \langle P_4 \rangle$$

observation angle by the sum of the four intensities. Spurious data points are rejected if they fall more than 2.5 sigma away from the values predicted by Eqs. 22–25.

The theoretical parameters, $\langle P_2 \rangle$, $\langle P_4 \rangle$ and $t$ (equal to $D$ times $\tau$) are then fitted to the data using a nonlinear least square regression analysis. Although the regression was slow, it did not encounter any local minima. All calculations were performed using a VAX 11/750 computer (Digital Equipment Corp, USA) with a floating point accelerator.

The derived results are also used for comparison to solution studies of the same probes bound to isotropic liposomes. The fluorescence anisotropy, $r$, is predicted using Eqs. (10 and 26–30). The vectors **e** and **o** are averaged over the surface of the sphere. The final result is:

$$r = \tfrac{2}{5}[H_0(\tau) + 2H_1(\tau) + 2H_2(\tau)]. \tag{39}$$

## RESULTS

### Experimental Artifacts: Sources and Correction

The majority of the artifacts in these experiments stem from changes in the light as it crosses the boundary between the lipid and surrounding medium. Since the refractive indexes are different, the light is refracted, reflected, and scattered at the interface. The extent of the alterations depends on the texture of the sample surface, the ratio of the two refractive indexes, the angle of incidence, and the polarization of the light.

Let us first consider the refraction and reflection of the light at the interface. Refraction is corrected using Snell's law (Jenkins and White, 1957):

$$\frac{\sin \phi_1}{\sin \phi_2} = \frac{n_1}{n_2} \tag{40}$$

The letter $n$ is the refractive index and the subscripts 1 and 2 refer to the surrounding medium and lipid, respectively. The angle $\phi$ is the angle between the light and the normal of the membrane.

Reflection of light at the interface is sensitive to the light's polarization. Fresnel's laws (Jenkins and White,

1957) are used to calculate for the light loss:

$$T_\parallel = 1 - \frac{\sin^2 (\phi_1 - \phi_2)}{\sin^2 (\phi_1 + \phi_2)} \tag{41}$$

$$T_\perp = 1 - \frac{\tan^2 (\phi_1 - \phi_2)}{\tan^2 (\phi_1 + \phi_2)}, \tag{42}$$

where $T$ is the amount of light transmitted at the interface. Parallel and perpendicular refer to the plane of the membrane.

An isotropic index of refraction of 1.47 for all lipid samples was selected based on results from DPPC below the phase transition in solution phase liposomes (Yi and MacDonald, 1973). This choice ignores possible errors introduced by alternate lipid compositions and different experimental wavelengths. Furthermore, some lecithins have an anisotropic refractive index (Cherry and Chapman, 1969; den Engelsen and de Konig, 1975). Calculations were performed to determine the errors that would arise from inaccuracies in the assumed value for the refractive index (Adler, 1985). The effect of birefringence
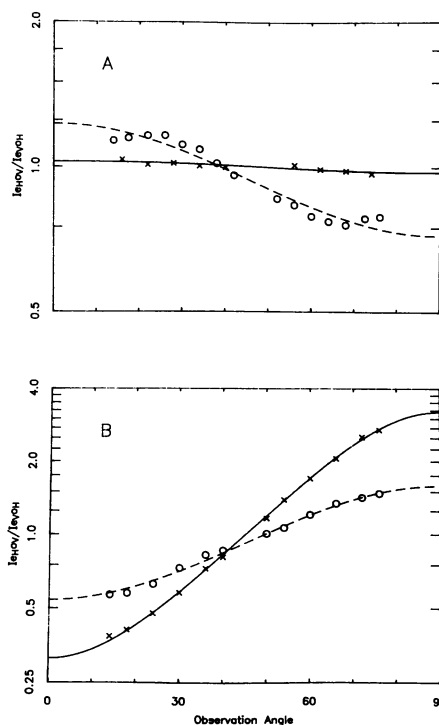


FIGURE 6 The Effect of Internal Reflection on the Data from DPH and Adriamycin. The plot of the ratio of $Ie_Ho_V/Ie_Vo_H$ verses observation angle: $a$ adriamycin and $b$ DPH in DPPC. The following symbols are used: O data from sample mounted on clear glass with the best fit of theoretical curve – –, × data from an identical sample mounted on black glass with the best fit of the theoretical curve ——. All intensities are corrected for the index of refraction. Deviation from the theoretical curves is more pronounced for adriamycin due to it its apparent isotropic motion. Although the data set from DPH on clear glass shows an acceptable fit, it was rejected because the results indicate that the emission and absorption dipoles are not parallel. This contradicts solution studies (Kawato et al., 1977; Lakowicz et al., 1979) as well as our own data.

was also considered. Our results indicate that the errors were less than or equal to the standard deviation between samples.

The errors introduced by light reflection are not limited to the front surface of the sample. A certain percentage of the light is also reflected at the rear surface. The distortions caused by this effect are graphically demonstrated in Fig. 6. Probes with relatively high anisotropy, such as DPH, tend to mask the problem. The uncorrected data shows an acceptable fit to a theoretical curve, even though the data yields erroneous results. For probes with lower anisotropy, adriamycin for example, the uncorrected data shows a poor fit to the theoretical curves. In both cases, the uncorrected data yields false results.

The problem is solved by forming the membranes directly on the surface of an opaque, or black, glass slide. The dye within the glass absorbs all the light which passes into the glass from the sample, thus preventing spurious reflection. The refractive index of the glass was approximately the same as the lipid bilayers (1.52 vs. 1.47). Therefore, no significant reflection of light is expected at the interface. Also it should be noted that prolonged illumination did not raise the temperature of the sample by more than 0.1°C.

A separate problem arises from scattering of light. To a certain extent, light scatter is a problem in all fluorescence depolarization measurements. However, due to the large size of the sample in the present studies, the intensity is several orders of magnitude greater than in the corresponding measurements on solution samples and additional optical filters are required. The experimental details are outlined in the methods section.

There are two other important sources of errors which are unrelated to changes in the refractive index. First, the results are very sensitive to the alignment of the sample vis-a-vis the fluorometer optics. As our sample alignment techniques improved, the random scatter in the data was reduced by three-fold. One must presume that systematic errors in alignment cause systematic deviations in the results.

A second, more difficult problem arises from dehydration of the experimental samples. It was demonstrated by Janiak et al. (1976, 1979) that ~25% water by weight is needed to maintain the normal bilayer structure. Special precautions were taken to insure proper hydration (see Methods) and temperature studies on the phase transition of DMPC indicated that we were successful. However, the one day old samples showed alterations in the data which may stem from hydration problems. Alternatively, the observed differences in the one day old samples may have been caused by changes in the packing of the membranes, such as the slow annealing of defects. Therefore, we do not feel we have conclusively solved this problem.

Two additional tests that assay the overall accuracy of the data were also performed. Control experiments were done with unoriented samples (Table IV). These samples

consisted of a fluorophore in solution. The solution is sandwiched between a clear microscope slide and the black glass support. Such a sample was used in lieu of the more preferable choice of an unoriented fluorophore dissolved in a lipid bilayer, because no such fluorophore was found. Three samples were selected. These were chosen to show increasing amounts of light scatter.

The experimental results from these controls agree with theory except for a small degree of order. The source of this is unknown, but may arise from light loss from scatter or adherence of the fluorophore to the glass surface. The light scatter from the sample itself has no effect on the results.

To further test the overall accuracy of the measurements, the experimental value for ratio $I_{xy}/I_{xx}$ is used to calculate the fluorescence anisotropy. This ratio is comparable with the value of $I_\perp/I_\parallel$, which assays the degree of anisotropy of solution phase samples. Our data show credible agreement with results obtained by standard techniques.

A second method was used to check the data. This approach derives a single experimental result from independent data sets. For the purposes of calculation, we assume that the transition dipoles are parallel to each
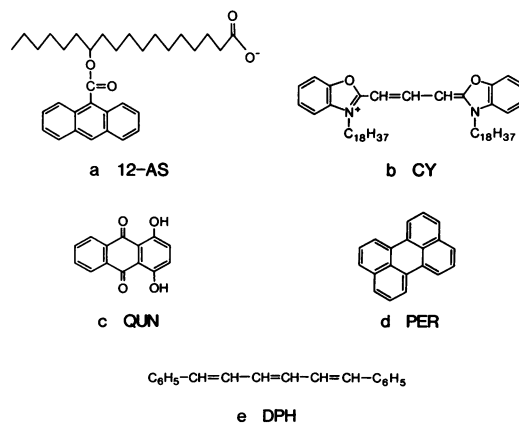


FIGURE 7 Structure of the Fluorescence Probes. The structures are labeled as follows: (*a*) 12-9-anthronyl-stearic acid (12-AS), (*b*) N,N'-di(octadecyl)oxacarbocyanine (CY), (*c*) Quinizarin (QUN), (*d*) Perylene (PER), and (*e*) 1,6-diphenyl-1,3,5-hexatriene (DPH).

other. The assumption is supported by measurements of $r_o$ on DPH (Kawato et al., 1977; Lakowicz et al., 1979) and the anthracylines (Burke and Tritton, manuscript submitted for publication) in isotropic solvents. For these results, the largest possible angle between the two dipoles is 5° and the maximum error introduced by this is ~5%. This is close to our normal experimental error.

If the transition dipoles are parallel, then $I_{zx}/I_{xz} = 1$. The value of $I_{zx}/I_{xz}$ have been derived from different experimental intensities. The results of more than 60 separate experiments show that for DPH the ratio is $0.96 \pm 0.05$ and for the anthracycline antibiotics it is $1.00 \pm 0.05$; both are in close agreement with the predicted value of $1.00 \pm 0.05$.

## Experimental Results with Various Fluorescent Probes

*DPH.* Our first experiments with conventional probes were performed with 1,6-diphenyl-1,3,5-hexatriene (DPH in Fig. 7). The physical properties of this fluorophore make it ideal for the study of membrane structure and motion. It is highly hydrophobic and partitions into the hydrocarbon core of the membrane. The molecule has a rod-like shape; its preferred orientation is parallel to the lipid side chains. The transition dipoles are parallel to the long axis of the molecule. This probe has been extensively used in fluorescence depolarization measurements of lipid bilayers in solution (Lakowicz et al., 1979; Stubbs et al., 1981; Kinosita and Ikegami, 1984) and oriented membranes (Frehland et al., 1982; Kooyman et al., 1981 and 1983; Vos et al., 1983).

In aqueous dispersions of saturated phosphatidylcholines, DPH senses the cooperative phase transition. Lakowicz and coworkers (1979) investigated this phenomenon with both steady-state and time-resolved fluorescence depolarization measurements. Their results demonstrated that $\langle P_2 \rangle$, the second degree order parameter, of DPH goes from 0.9, in the gel phase, to 0.3, in the liquid-crystal phase. As expected, the change was highly cooperative.

Our results from temperature studies with DPH in DMPC and DPPC are presented in Figs. 8 and 9. The data indicate that the second degree order parameter increased through the phase transition (Fig. 8 *a* and 9 *a*). Furthermore, there was no evidence of a cooperative phase transition. This result is distinctly different than the comparable data from solution measurements. The variations in $\langle P_4 \rangle$ were similar to those seen in $\langle P_2 \rangle$, but the changes occurred over a greater range (Fig. 8 *b* and 9 *b*). As expected, the rate of rotation increased with temperature (Fig. 8 *c* and 9 *c*) and there was no abrupt change at the phase transition, in agreement with the results of other authors (Lakowicz et al., 1979; Kinosita and Ikegami, 1984).

We have examined several aspects of the experimental protocols in an attempt to explain the differences in the values of $\langle P_2 \rangle$ observed in our system when compared with
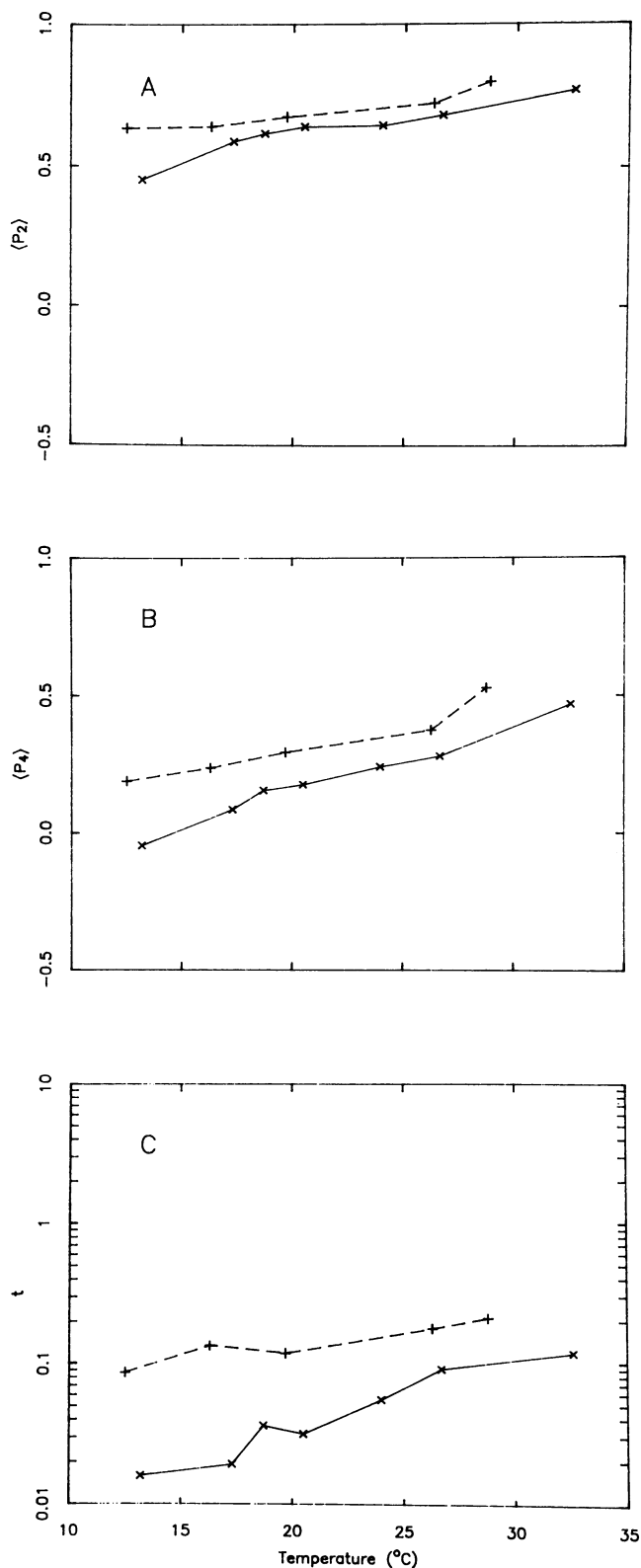


FIGURE 8  The Effect of Temperature on the Rotational Dynamics of DPH in DMPC. The two lines represent separate experiments. The samples were selected from the same batch, but used on different days. The $X$'s connected by —— are from the first experiment. The second experiment, represented by the +'s connected with – –, was run two days latter. The order parameters are higher for this data set and the rotational rates are faster. This trend was observed for most of the older membranes irrespective of the probe.

The parameters are displayed in the following graphs (*a*) $\langle P_2 \rangle$, (*b*) $\langle P_4 \rangle$, and (*c*) the angular diffusion rate (rad/s) times the fluorescence lifetime. The fluorescence lifetime of DPH bound to aqueous dispersions of membranes is approximately 9 ns (Lakowicz et al., 1979).
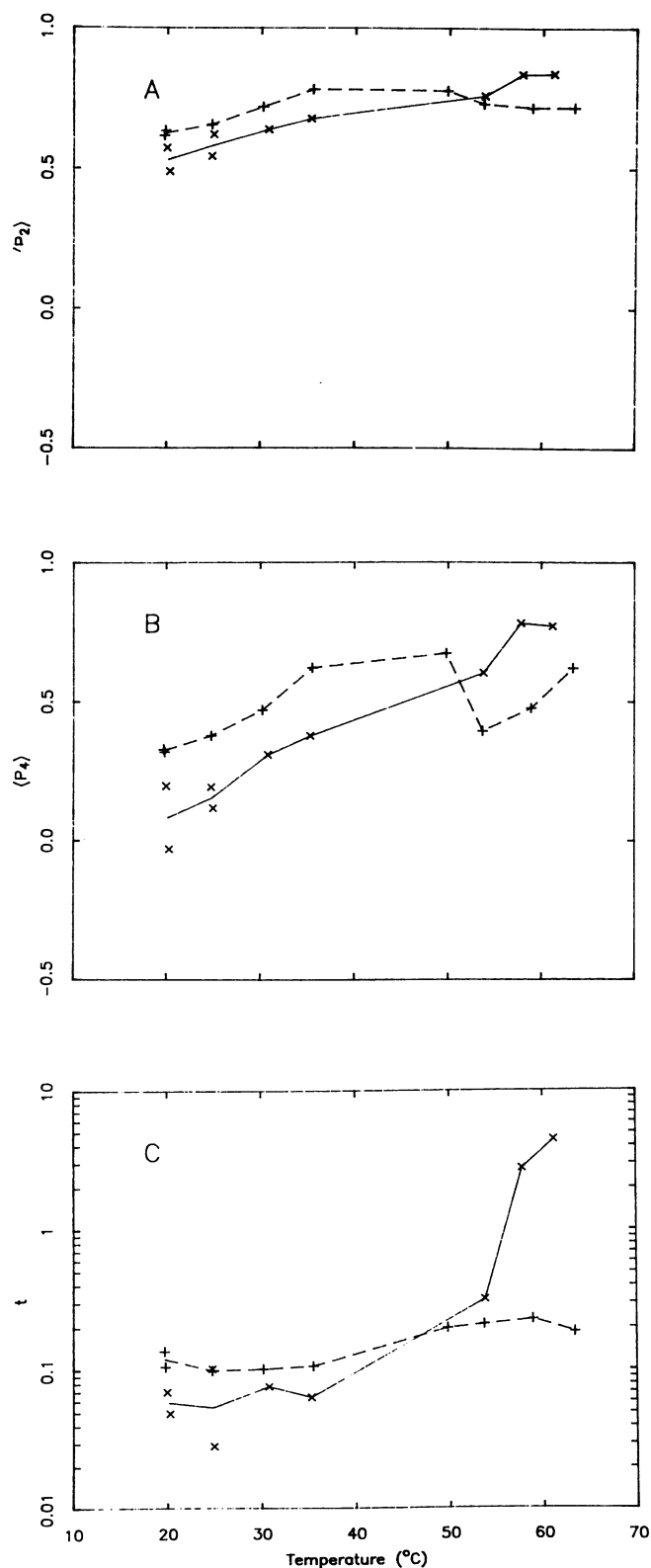
solution studies. First, the data was re-analyzed using alternate modeling assumptions (see Discussion section). There were minor shifts in the results, but the trends remained unchanged (Adler, 1985). This is not surprising since the raw data itself does not reflect the cooperative phase transition.

Another possibility is that the membranes were severely dehydrated. This would shift or obscure the phase transition (Janiak et al., 1976, 1979). We sought an independent verification that the membranes underwent a cooperative phase transition. The amount of light scatter (470 nm) was monitored in parallel with the total fluorescence intensity (360 nm). The polarizers were removed from the fluorometer and the sample alignment was left unchanged during these measurements.

The data from both wavelengths indicate that the lipids undergo a cooperative phase transition (data not shown). In DPPC, the phase transition occurred at higher than normal temperatures and was apparently irreproducible without rehydrating the membranes, thus indicating that the membranes became dehydrated at the higher temperatures. Therefore, the results from this lipid must be treated with some caution. The DMPC membranes underwent a reversible phase transition at the appropriate temperature (21°C). The data demonstrate a cooperative change near the normal transition temperature. Furthermore, the results from the total fluorescence intensity demonstrate that the probe senses the transition.

Both $\langle P_2 \rangle$ and $\langle P_4 \rangle$ increased with temperature. This change may reflect alterations in tilt of the lipid side chains. This tilt has been estimated to be 30° in the gel phase (Janiak et al., 1976). The chain tilt disappears above the phase transition and the probe would preferentially reorient parallel to the membrane normal.

We remain puzzled by the discrepancies between our results and reported values of $\langle P_2 \rangle$ obtained from solution measurements of DPH in similar lipids (Lakowicz et al., 1979; Stubbs et al., 1981; Kinosita and Ikegami, 1984). Our additional measurements with a broad range of probes (see, for example, the following section on anthracycline antibiotics) showed a close correlation between the value of the fluorescence anisotropy, $r$, calculated from our data using Eq. 39, and the value of $r$ measured in sonicated liposomes. This indicates that the general approach is sound and the oriented membranes are structurally similar to the single bilayers present in sonicated liposomes. However, the anomalous differences between the results from DPH dissolved in oriented membranes and the isotropic dispersions represent a special case.

Below the phase transition, lower than expected values of $\langle P_2 \rangle$ were observed for DPH in both DMPC and DPPC. This may have resulted from inherent differences in $\langle P_2 \rangle$ as measured in these results compared with $\langle P_2 \rangle$ derived from isotropic dispersions. In our studies the order parameters are measured relative to the normal of the membrane; in isotropic dispersions the order parameters are measured

FIGURE 9 The Effect of Temperature on the Rotational Dynamics of DPH in DPPC. The two lines represent separate experiments. The $X$'s connected by —— are from an experiment with controlled humidity. The $+$'s connected with – – come from a second experiment in which no precautions were taken to insure proper hydration. Therefore, the data is less accurate. The rotational parameters are displayed in the following graphs (a) $\langle P_2 \rangle$, (b) $\langle P_4 \rangle$, and (c) the angular diffusion rate (rad/s) times the fluorescence lifetime.

relative to the axis of the probe. If the probe has an average tilt away from the membrane, then a lower value of $\langle P_2 \rangle$ would be observed in oriented membranes than in solution, just as we find.

$\langle P_2 \rangle$ increased above the phase transition in the oriented membranes. This contrasts with solution phase measurements which show $\langle P_2 \rangle$ falling rapidly above the phase transition as the acyl side chains melt, leading to a disordered packing of the membrane. There is no simple mathematical or theoretical explanation for the observed discrepancies between our results and those of previous investigators. Instead, the data suggest that there are structural differences between the environment or binding of DPH in oriented membranes and in isotropic dispersions. It is not likely that differences in membrane curvature lead to this effect, since order parameters for multilamellar liposomes (Stubbs et al., 1981) are only slightly higher than those measured on unilamellar vesicles (Kinosita and Ikegai, 1984). Possibly, the isotropic dispersions are more flexible than the stacked planar membranes used in these studies. Alternatively, structural alterations may arise from hydration effects. The reproducibility of the results over many separate experimental determinations convinces us that the data and calculations are correct. However, we can offer no single explanation which completely explains all the observed results.

*Other Conventional Probes.* Experiments were also performed with other conventional probes (Table V). Many of the experiments were chosen to explore the sensitivity of the technique. The following conclusions were reached.

(*a*) $\langle P_2 \rangle$ ranged from 0.8 to $-0.4$, spanning 80% of the theoretically possible values. This demonstrates that the technique is sensitive to a wide range of orientations. More extreme values of $\langle P_2 \rangle$ are probably excluded by random thermal motion.

(*b*) Simultaneous measurements at a second wavelength were made for two of the probes, perylene and 12-AS. For perylene, the shorter wavelength excites the same transitions. As expected, the two data set were nearly identical. This shows the results are independent of the exciting wavelength.

For 12-AS, the shorter wavelength excites a second transition. The transition dipoles shift from a parallel orientation to a mutually perpendicular conformation, at the shorter wavelength. Therefore, the fluorescent light is depolarized in the absence of molecular motion. This depolarization of the light would lead to an apparent decrease in order. The lower values of $\langle P_2 \rangle$ and $\langle P_4 \rangle$ reflect this expectation.

(*c*) The negative values for $\langle P_2 \rangle$ measured with 12-AS and CY are expected on structural grounds. Negative values of $\langle P_2 \rangle$ imply that the transition dipoles are more closely oriented with the plane of the membrane. The transition dipoles of 12-AS are parallel to the short axis of the molecule. For CY, the hydrophobic octadecyl side chains anchor the molecule to the bilayer and the fluorophore is parallel to the plane of the membrane.

The data also invite certain comparisons between the

### TABLE V
### CONVENTIONAL PROBES

| Probe | $\langle P_2 \rangle$ | $\langle P_4 \rangle$ | $t$ | Ring angle | Power | $k$ | $r$ |
|---|---|---|---|---|---|---|---|
| DPH in DMPC 17° | 0.63 | 0.17 | 0.05 | 33° | 3.7 | 3.4 | 0.34 |
| DPH in DMPC 27° | 0.77 | 0.44 | 0.08 | 31° | 1.8 | 4.0 | 0.31 |
| DPH in DPPC 25° | 0.67 | 0.31 | 0.07 | 37° | 2.0 | 3.1 | 0.31 |
| DPH in DPPC 54° | 0.76 | 0.46 | 0.23 | 31° | 1.5 | 3.8 | 0.28 |
| DPH in Egg Lecithin | 0.20 | 0.15 | 0.16 | 57° | 0.25 | 2.7 | 0.24 |
| PER @ 441 nm in DPPC | 0.48 | 0.24 | 0.14 | 47° | 0.83 | 2.4 | 0.24 |
| PER @ 394 nm in DPPC | 0.49 | 0.25 | 0.13 | 46° | 0.83 | 2.7 | 0.25 |
| 12-AS @ 385 nm in DPPC | −0.22 | 0.07 | 0.18 | 70° | 0.32 | 2.1 | 0.20 |
| 12-AS @ 347 nm in DPPC | −0.16 | 0.05 | 0.13 | 63° | 6.7 | 2.2 | 0.23 |
| 12-AS @ 385 nm in EL | −0.05 | 0.07 | 0.34 | 60° | 0.10 | 1.6 | 0.14 |
| CY in DPPC | −0.42 | 0.01 | 0.15 | 77° | 6.0 | 17 | 0.27 |
| QUN in DPPC | 0.19 | 0.13 | 0.30 | 56° | 0.27 | 2.5 | 0.16 |
| Average standard deviation | ±0.04 | ±0.04 | ±0.03 | ±1.3° | ±0.4 | ±0.5 | ±0.015 |

$\langle P_2 \rangle$, $\langle P_4 \rangle$ and $t$: $\langle P_2 \rangle$ and $\langle P_4 \rangle$ are the second and fourth degree order parameters. $t$ is the product of fluorescence lifetime (second) and the rate of rotation.

Ring Angle: This gives best approximation of the average tilt angle. It should only be used for comparison between samples because it does not accurately reflect the motion of the probe.

Power and $k$: These two parameters describe the average orientation of the probe. $k$ gives the energy difference, in kcal/mol, between the least and most favorable orientations of the probe. The power is equivalent to the factor $p$ in Eq. 47. It describes the shape of the angular distribution. The smaller the value of the power, the sharper the distribution.

$r$: This is the predicted value for the fluorescence anisotropy from a solution phase experiment.

Average Standard Deviation: This is obtained from repeat samples of the same preparation. All measurements were performed on the same day. The values are the average from all the probes.

structure of different lecithins and the binding properties of the probes:

(d) The probes were more oriented in saturated phosphatidyl cholines than in unsaturated egg lecithin (Table V, 12-AS and DPH). Also the rotational rates were higher in egg lecithin. This implies that the side chains of egg lecithin are more disordered. This undoubtedly arises because the double bonds and unmatched chain length of egg lecithin disrupt the packing of the hydrocarbon core.

(e) The motion of DPH is very similar in the liquid–crystal (fluid) phases of the saturated lecithins DMPC and DPPC. The slower rate of rotation in DMPC reflects the different temperature ranges used in the two experiments (10°C–35°C for DMPC and 20°C–65°C for DPPC).

Below the phase transition the values of $\langle P_2 \rangle$ for DPH in the two lipids are similar. There is a marked difference in the value of $\langle P_4 \rangle$. The smaller value of $\langle P_4 \rangle$ for DMPC indicates a broader spatial distribution. DMPC was in the pretransition phase. The spatial distribution may reflect the ridges observed in pretransition phase membranes (Janiak et al. 1976, 1979).

(f) In general, probes are oriented by long hydrophobic regions in their structure. The longer the hydrophobic region the greater the orientation. The octadecyl side chains of CY firmly anchor it to the membrane ($\langle P_2 \rangle = -0.43$).[2] Amongst the aromatic probes, DPH is longer and more oriented than perylene ($\langle P_2 \rangle$ values of 0.69 and 0.45 respectively).

(g) The probes with groups that potentially can form hydrogen bonds are more disordered. Quinizarin is a dihydroxylanthraquinone ($\langle P_2 \rangle = 0.19$). It is relatively unoriented compared with the other probes. The carboxyl group of 12-AS ($\langle P_2 \rangle = -0.16$) makes it more disordered than perylene or DPH.

## Anthracycline Antibiotics

The anthracycline antibiotics are frequently used in the treatment of cancer (Arcamone, 1981; Young et al., 1981; Gianni et al., 1984). Adriamycin, clinically the most important member of this group, is part of many chemotherapeutic regimens. Most anthracyclines intercalate into double stranded DNA, thus interfering with its template function. Many investigators have stated that this interaction is the basis of the antineoplastic action. However, further research has raised doubts about this hypothesis and a growing body of evidence indicates that anthracyclines exert their antineoplastic action by disrupting the function of cytoplasmic membranes. These drugs modify physical and biological properties of the membranes (reviewed by Tritton and Hickman, 1985) and are cytotoxic

to neoplastic cells without penetrating beyond the plasma membrane (Tritton and Yee, 1982; Tritton et al., 1983; Wingard et al., 1984; Tokes et al., 1982; Rogers et al., 1983) suggesting that the plasma membrane is at least part of adriamycin's primary target.

One approach to studying the membrane binding mechanism of the anthracyclines is to make comparisons between closely related analogues. By examining effects of single changes in functional groups, one can observe the interplay between drug structure and rotational dynamics. The lipid L-α-dipalmitoyl phosphatidyl choline (DPPC) was selected for these studies, because the anthracyclines bind more tightly to gel phase bilayers (Burke and Tritton, 1984) and the drugs are more likely to partition into the more solid regions of natural membranes.

The results for ten different anthracyclines are given in Table VI. The molecule 1,4-dihydroxyl-9,10-anthraquinone, or quinizarin, is included for comparison.

The first section of the table displays results from modifications in the aglycone ring. The analogues daunomycin, carminomycin and 4-demethoxy-daunomicin are identical except for the constituent attached to the C4 of the anthraquinone (Fig. 10). These modifications have a potent effect on the drugs' orientation. Results from daunomycin and adriamycin indicate that the group attached to the alicyclic ring through the C13 carbonyl has a smaller effect on the rotational dynamics. This was expected due to the close similarity in the fluorescence properties of these analogues when bound to solution phase liposomes (Burke and Tritton, 1985a, b).

Modification of the sugar residue had a more varied effect on the orientation of these compounds. For daunomycin, both methylation of the amino group as well as the removal of the sugar increased the order parameters. For adriamycin, changes in the sugar had little effect, but the total removal of the sugar caused a pronounced increase in the order parameters.

The complex relationship between sugar structure and orientation is not surprising. Solution studies with gel phase bilayers have indicated that the sugar group influences both electrostatic and hydrophobic interactions (Burke and Tritton, 1985a, b). Thus, any single modification in the sugar could have multiple consequences on drug orientation.

The results from the analogues are consistent with the following interpretation. The C4 carbon is buried in the bilayer. Hydrophilic substitutions on this carbon tend to disrupt the membrane interaction. The C13 carbon and the sugar are located near the phospholipid head groups. Substitutions here have little interaction with the interior side chains.

We also studied the effects of lipid composition on drug binding and the findings are reported in Table VI. There are significant differences in the rotational dynamics of adriamycin in all three phases of saturated phosphatidylcholines. These phases are, in order of increasing tempera-

---

[2]The positive values of $\langle P_2 \rangle$ range from 1, for complete order, to 0, for a random conformation. The negative values range from $-0.5$ to 0. Therefore, an order parameter of $-0.43$ is roughly comparable with one of $+0.86$.

TABLE VI
ANTHRACYCLINE ANTIBIOTICS: ALL PROBES ARE IN DPPC AT ROOM TEMPERATURE

| Probe | $\langle P_2 \rangle$ | $\langle P_4 \rangle$ | $t$ | Ring angle | Power | $k$ | $r$ |
|---|---|---|---|---|---|---|---|
| Modifications of the aglycone | | | | | | | |
| Adr | 0.02 | 0.01 | 0.11 | 59° | 0.12 | 0.48 | 0.26 |
| Dau | −0.02 | 0.01 | 0.11 | 61° | 0.26 | 1.7 | 0.26 |
| Car | 0.23 | 0.13 | 0.10 | 56° | 0.34 | 2.2 | 0.26 |
| Met-Dau | 0.30 | 0.09 | 0.17 | 50° | 1.1 | 1.3 | 0.22 |
| Qun | 0.19 | 0.13 | 0.30 | 56° | 0.26 | 2.4 | 0.16 |
| Modifications of the amino sugar | | | | | | | |
| Adr | 0.02 | 0.01 | 0.11 | 59° | 0.12 | 0.48 | 0.26 |
| Adr-ag | 0.39 | 0.18 | 0.07 | 51° | 0.78 | 3.6 | 0.29 |
| Epi-adr | 0.2 | −0.01 | 0.12 | 58° | 8.3 | 0.05 | 0.26 |
| N,N-adr | 0.04 | 0.05 | 0.08 | 63° | 0.09 | 1.7 | 0.29 |
| Dau | −0.02 | 0.01 | 0.11 | 61° | 0.26 | 1.7 | 0.26 |
| Dau-ag | 0.25 | 0.14 | 0.10 | 56° | 0.38 | 2.3 | 0.26 |
| N,N-dau | 0.31 | 0.15 | 0.09 | 54° | 0.60 | 2.0 | 0.27 |
| Adriamycin in different lipids at room temperature | | | | | | | |
| DPPC | 0.02 | 0.01 | 0.11 | 59° | 0.12 | 0.48 | 0.26 |
| DMPC at 18° | 0.46 | 0.09 | 0.07 | 44° | 3.7 | 2.0 | 0.29 |
| DMPC at 26° | 0.47 | 0.21 | 0.08 | 46° | 1.3 | 2.2 | 0.27 |
| Egg lecithin | −0.02 | 0.01 | 0.033 | 63° | 0.16 | 0.42 | 0.34 |
| DPPC | 0.02 | 0.01 | 0.11 | 59° | 0.12 | 0.48 | 0.26 |
| DPPC + .5% CL | −0.19 | −0.17 | 0.16 | 65° | 23 | >10 | 0.22 |
| DPPC + 1% CL | 0.02 | 0.01 | 0.13 | 59° | 0.12 | 0.48 | 0.26 |
| DPPC + 2% CL | 0.16 | 0.07 | 0.13 | 56° | 0.40 | 1.4 | 0.23 |
| DPPC + 3% CL | 0.29 | 0.11 | 0.12 | 52° | 0.81 | 1.5 | 0.24 |
| Average standard deviation | ±0.04 | ±0.04 | ±0.03 | ±1.3° | ±0.4 | ±0.5 | ±0.015 |

See Legend for Table V.

ture: the gel (solid) phase, pretransition phase, and the liquid-crystal (fluid) phase (Janiak et al., 1976, 1979; Mabrey and Sturtevant, 1978). The hydrocarbon core of the membrane is highly ordered in both the gel and pretransition phases. The major difference between the two is that ridges form in the lipid in the pretransition phase (Janiak et al., 1976, 1979). At higher temperature, the hydrocarbon core melts and becomes more disordered. This is the liquid-crystal phase. In the gel phase the order parameters of adriamycin are very low ($\langle P_2 \rangle$ = 0.02 in DPPC @ 25°). $\langle P_2 \rangle$ increases significantly in the pretransition phase ($\langle P_2 \rangle$ = 0.4 in DMPC @ 18°). Above the phase transition, in the liquid-crystal phase, $\langle P_2 \rangle$



| Compound | R₁ | R₂ |
|---|---|---|
| DAUNOMYCIN | OCH₃ | CH₃ |
| 4-DEMETHOXYDAUNOMYCIN | H | CH₃ |
| CARMINOMYCIN | OH | CH₃ |
| ADRIAMYCIN | OCH₃ | CH₂OH |

FIGURE 10 Structure of the Anthracyclines.

decreases but $\langle P_4 \rangle$ increases (DMPC @ 26°). This phase behavior is significantly different than the probe DPH and may reflect the amphipathic properties of the drug.

In a separate experiment, the order parameters of adriamycin in egg lecithin were found to be near zero (Table VI). This reduction in order is similar to the results obtained with 12-AS and DPH.

The research was extended to include studies of membranes with a small percentage of cardiolipin (CL). This lipid has a powerful modulating effect on the interaction between adriamycin and synthetic membranes (Tritton et al., 1978; Murphee, et al., 1982). The results confirm there is an unique interaction between adriamycin and membranes containing cardiolipin. At an equimolar concentration of both compounds (0.5% CL by weight, 1/400 drug-lipid ratio) adriamycin has a negative value for both $\langle P_2 \rangle$ and $\langle P_4 \rangle$. The large negative value of $\langle P_4 \rangle$ is particularly unusual and has not been seen with any other probe. The values of $\langle P_2 \rangle$ and $\langle P_4 \rangle$ increase as the concentration of cardiolipin increases.

It is important to note that the data at 1% CL are identical to results with 0% CL. The order parameters are near zero in both cases and the simplest interpretation is that the drug is randomly oriented under these conditions. However, this conclusion seems unlikely considering the overall trends. A second interpretation is that the drug has multiple orientations, and the order parameters of the
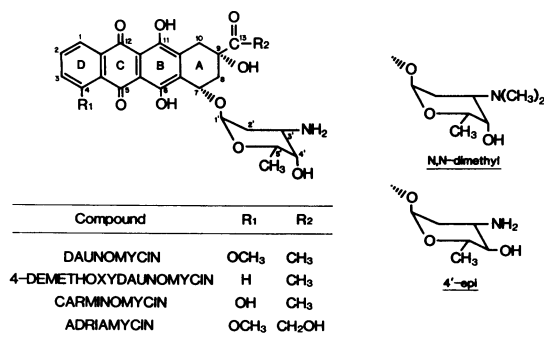
resulting combination are near zero. Consistent with this interpretation, other physical techniques have indicated there are multiple binding sites for the anthracyclines under certain conditions (Burke and Tritton, 1985a, b).

Finally, there is good correlation between the fluorescence anisotropy, r, measured in solution (Burke and Tritton, 1985a, b) and from globally oriented membranes (see Eq. 39). The two sets of data demonstrate similar trends, indicating that the experimental systems are very similar. On the average the value of r measured in the globally oriented membranes was slightly lower (0.03 ± 0.01). The smaller values may reflect an increase in the fluorescence lifetime of the anthracyclines in oriented membranes.

## DISCUSSION

### Models

It was once thought that small molecules rotated isotropically in membranes. Lipids created a viscous drag on the molecule that reduced the rate of rotation, but they did not alter the molecule's course. The experimental data was interpreted in terms of the Perrin equation. The microviscosity of the probes environment was derived from the single parameter data.

Technical improvements made it possible to perform time resolved measurements of fluorescence. Such results conclusively showed that most probe motion was anisotropic. The Perrin model was rejected in favor of two parameter models: the first parameter was a measure of the degree of anisotropy and the second gave the rate of rotation.

The experiments presented here are made in an anisotropic fashion, i.e., the orientation of the bilayer in the laboratory frame is known. Three independent parameters are derived from the data. One parameter assays the rate of rotation and the other two describe the angular distribution of the probe. Our results demonstrate that the previous two parameter models should thus be updated.

In general, a model for a probe's motion is accepted or rejected based on its ability to simulate the experimental data. The accuracy of the simulation is assayed by the root mean square error (RMS) between the calculated and real values of the data. The values of the RMS are compared with the RMS calculated from a four parameter model. As a general rule, a 5% increase in the RMS is considered to be the break point where further parameters yield no improvement.

### Selecting the Number of Independent Parameters

As was explained in the section on mathematical analysis, a maximum of six independent numbers are needed to simulate the fluorescence intensities. One of these must be used to normalize the data. Another one is lost if the absorption and emission dipoles are parallel to each other. (The experimental data justify this assumption for both DPH and the anthracyclines.) Therefore, we are left with four independent numbers.

Of course, experimental considerations may further limit the number of independent parameters. As an example, the motion of an isotropic probe is described by one parameter, the rotational diffusion constant.

Our results demonstrate that three and only three parameters are needed to simulate the data. The RMS increases by about two to five-fold for various two parameter models. The average increase in the RMS between the three and four parameter models is only 2%. The three parameter model uses the second and fourth degree order parameters and the rotational rate. The four parameter model uses $\langle P_2 \rangle$ and the three correlation coefficients. This increase in the RMS between the three and four parameter models is negligible, and it confirms the accuracy of Szabo's (1984) approximations of the correlation coefficients.

However, the apparent agreement between the three and four parameter models may reflect practical and not theoretical considerations. Two of the four independent parameters are derived from the intensity $Ie_Ho_H$. The data from this intensity may not be sufficiently accurate to distinguish between three and four parameter models. Technical improvements are required in order to reach a decisive conclusion on this matter.

Given the resolution of current techniques, the three parameter model gives an acceptable fit to the data and is used in all of the subsequent discussion.

### Interpreting $\langle P_2 \rangle$ and $\langle P_4 \rangle$

The second and fourth degree order parameters, $\langle P_2 \rangle$ and $\langle P_4 \rangle$, are derived independent of any model for the probe motion. Therefore, they are not subject to errors in the modeling assumption. Unlike previous models for probe motion, the results should not require revision, even if a new technique that provides more information is subsequently developed. However, quantitative interpretation of these parameters is more difficult.

$\langle P_2 \rangle$ and $\langle P_4 \rangle$ are part of an infinite series (Eq. 34). If all the terms are known, then the angular distribution function, $P(\beta)$, can be calculated. This function gives the number of molecules that are tilted at a given angle $\beta$. Unfortunately, the experimental results on steady-state fluorescence polarization yield no information on the higher order terms and $P(\beta)$ must be approximated from limited information. This approximation is equivalent to a model for the probe's orientation. Furthermore, the model restricts the range of $\langle P_2 \rangle$ and $\langle P_4 \rangle$ (Eq. 33). Models are rejected if experimentally observed order parameters consistently fall outside the range of the simulation.

Two different models with only two adjustable parameters, a rate of rotation and an orientational variable, were tested. The first was the nutating cone model. The probe freely diffuses inside a cone with a maximum angle of $\theta$. This model has been used in the literature to describe the

motion of small molecules in membranes (Berliner, 1976; Lakowicz et al., 1979; Stubbs et al., 1981; Kinosita and Ikegami, 1984). The second model, referred to as the ring model, was also tested. In this model the azimuthal angle $\beta$ is set to a fixed value. Neither model can adequately simulate the data (Fig. 11 *a*). It is interesting that the paramagnetic resonance detected motion of nitroxide spin probes in oriented membranes has usually been described by these types of simple models (see Berliner, 1976); our results suggest that it might be fruitful to consider other kinds of models for these results as well.

Zannoni et al. (1983) suggested the following angular distribution function:

$$P(\beta) = \frac{\exp(-U(\beta)/kt)}{\int_0^{\pi/2} \exp[-U(\beta)/kt] \sin \beta \, d\beta}, \qquad (43)$$

where $U(\beta)$ is the effective energy potential for a given azimuthal angle $\beta$. Defining an angular distribution in this way insures that $P(\beta)$ is always positive. However, the resulting equations become difficult to integrate in closed form and numerical integration and nonlinear regression must be used to solve for the adjustable parameters.

We tested three different models for the energy distribution $U(\beta)$. They were:

$$U(\beta) = c_2 P_2(\cos \beta) + c_4 P_4(\cos \beta) \qquad (44)$$

$$U(\beta) = k(\sin^2 \beta - \sin^2 \beta_{max})^2 \qquad (45)$$

$$U(\beta) = k|\sin \beta|p \quad \text{for } \langle P_2 \rangle > 0$$
$$= k|\cos \beta|p \quad \text{for } \langle P_2 \rangle < 0. \qquad (46)$$

The first, developed by Zannoni et al. (1983) and used by Kooyman et al. (1981, 1983), expresses the potential energy as a linear combination of the second and fourth degree Legendre polynomials of cos $\beta$. The distribution function is flexible enough to describe the majority of the probes (Fig. 11 *b*). However, for many probes the distribution function has two maxima. This implies that there are two binding sites. We are accordingly hesitant to put this claim forward in the absence of further supporting evidence.

Eqs. 45 and 46 were developed for this work. Each has a single maximum. Both models are subsets of the following three variable equation:

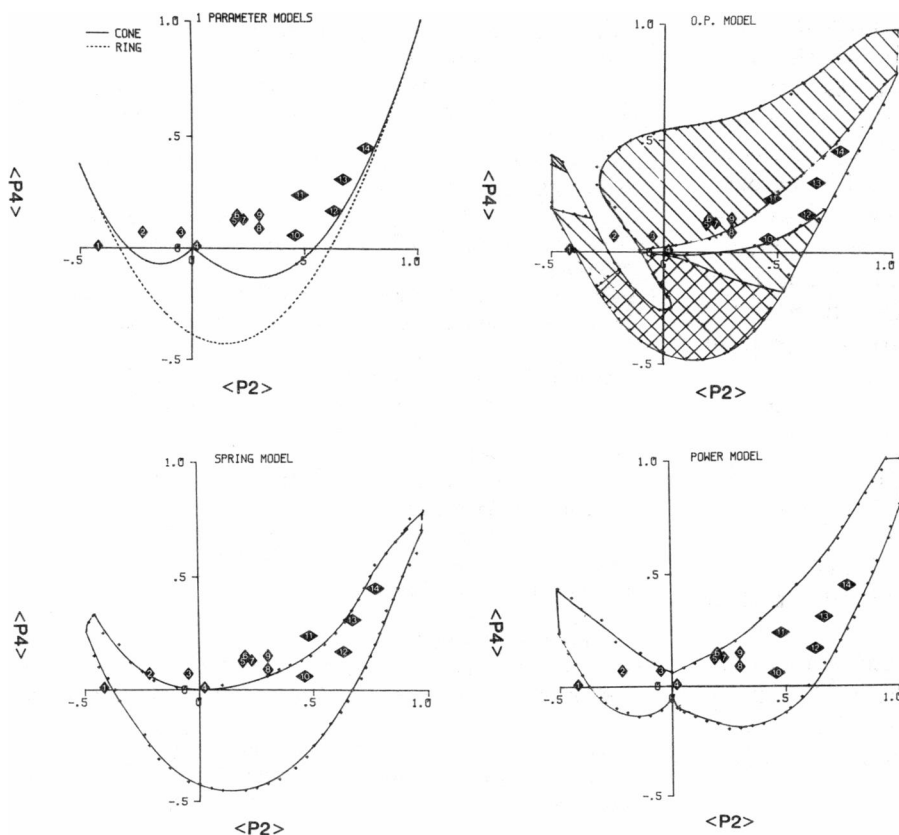$$U(\beta) = k|\sin^2 \beta - \sin^2 \beta_{max}|^p, \qquad (47)$$



FIGURE 11 The Range of the Order Parameters Encompassed by Various Models. The ranges of models, except panel *a*, lie within the marked boundaries. The small numbers surrounded by diamonds represents the $\langle P_2 \rangle$ and $\langle P_4 \rangle$ of the probes listed below. A plot of the $P(\beta)$ function for many of the probes appears in Fig. 5.

| No. | Probe | Lipid | Temperature |
| --- | --- | --- | --- |
| 1 | CY | DPPC | 25° |
| 2 | 12-AS | DPPC | 25° |
| 3 | 12-AS | E.L. | 25° |
| 4 | ADR | DPPC | 25° |
|  | Epi-ADR | DPPC | 25° |
|  | N,N-ADR | DPPC | 25° |
| 5 | QUN | DPPC | 25° |
| 6 | DPH | E.L. | 25° |
| 7 | Car | DPPC | 25° |
|  | DAU-AG | DPPC | 25° |
| 8 | MET-DAU | DPPC | 25° |
| 9 | N,N-DAU | DPPC | 25° |
| 10 | ADR | DMPC | 18° |
| 11 | PER | DPPC | 25° |
| 12 | DPH | DMPC | 17° |
| 13 | DPH | DPPC | 25° |
| 14 | DPH | DMPC | 27° |
|  | DPH | DPPC | 54° |

(*a*) Two single parameter models. — Nutating Cone Model. – – Ring Model. Since these models have a single orientational parameter, the value of $\langle P_2 \rangle$ determines the value of $\langle P_4 \rangle$. Only the values of $\langle P_2 \rangle$ and $\langle P_4 \rangle$ that fall directly on the line are consistent with the model. (*b*) Eq. 44. The different shading refers to the following types of the distribution: no shading — single maximum in the distribution function, centered on the membrane normal $\backslash\backslash\backslash\backslash\backslash\backslash\backslash$ — two maxima, one centered on the membrane normal and the other centered parallel to the plane of the membrane. $\times\times\times\times\times\times\times$ — single maximum, tilted away from the membrane normal. (*c*) Eq. 45, the spring model. (*d*) Eq. 46, the power model.

where $k$ is the maximum energy difference between the most and the least favorable orientations. $\beta_{max}$ is the angle with the highest concentration of probes. The constant $p$ describes how sharp the change in energy is near the maximum. Smaller values of $p$ imply a more narrow distribution near $\beta_{max}$.

The variable $p$ is set to 2 in Eq. 45. This equation was selected because it mimics a harmonic energy distribution. Unfortunately, the function is not very useful due to its limited range (Fig. 11 $c$). These results demonstrate that most small molecules in lipid bilayers are subject to more complex forces.

For Eq. 46, $\beta_{max} = 0°$ when $\langle P_2 \rangle > 0$ and $\beta_{max} = 90°$ when $\langle P_2 \rangle < 0$. This implies that the probe is oriented either parallel or perpendicular to the membrane normal. The model is flexible enough to describe almost all of the experimental data (Fig. 11 $d$). A plot of several different distributions appears in Fig. 5.

We also tested two additional models for the probability distribution. These relatively simple models did not use an energy distribution and they allowed $\beta_{max}$ to vary between 0° and 90°. Neither of these models successfully simulated the data.

Of all the models tested, only the power model gives a reasonable description of the probes motion. This model assumes that $\beta_{max}$, the center of the angular distribution, is either at 0° for $\langle P_2 \rangle > 0$ or at 90°, if $\langle P_2 \rangle < 0$. The model fits nearly all the data. The implication is that the most stable orientation for the probes[3] is with the long axis parallel to the membrane normal. (The only exceptions are CY in DPPC and adriamycin in DPPC + 0.5% cardiolipin.) The variation in the order parameters stems from differences in the energetics of rotation. The two adjustable parameters in this model are the total force opposing rotation and how rapidly this force changes with the angle. The results imply that the membrane restricts the probe to either perpendicular or parallel orientations.

The experimental source of these modeling constraints comes from the positive values of $\langle P_4 \rangle$ obtained for almost all probes. $\langle P_4 \rangle$ is positive when the angle $\beta$, the polar angle, lies between either 0° and 30° or 70° and 90°, ie, the probe is closely aligned with the coordinate axes.

The results indicate that the probes do not have an average tilt, i.e., $0° < \beta_{max} < 90°$. There is an important exception to this. Eq. 45, which mimics a harmonic oscillator, is consistent with the motion of diphenylhexatriene (DPH) in saturated lecithins. In many ways, DPH is the simplest probe studied. It has a long rod like shape and no hetroatoms. It is comforting that the motion of DPH is

explained by a simple physical model. Probes with even slightly more complex structures, such as perylene, no longer fit this model.

## REFERENCES

Adler, M. 1985. Thesis, Yale University, New Haven, Conn.

Arcamone, F. 1981. Doxorubicin, Anticancer Antibiotics, Medicinal Chemistry. vol 17. Academic Press, Inc., New York.

Badley, R. A. 1976. *Modern Fluorescence* 2:91–139.

Badley, R. A., H. Schneider, and W. G. Martin. 1971. Orientation and motion of a fluorescent probe in model membranes. *Biochem. Biophys. Res. Commun.* 45:174–183.

Badley, R. A., W. G. Martin, and H. Schneider. 1973. Dynamic behavior of fluorescent probes in lipid bilayer model membranes. *Biochemistry.* 12:268–275.

Berliner, L. J. 1976. Spin Labeling: Theory and Applications. Academic Press Inc., New York.

Burke, T., and T. R. Tritton. 1985a. Structural basis of anthracycline selectivity for unilamellar phosphatidylcholine vesicles: an equilibrium binding study. *Biochemistry.* 24:1768–1776.

Burke, T., and T. R. Tritton. 1985b. Location and dynamics of anthracyclines bound to unilamellar phosphatidylcholine vesicles. *Biochemistry.* 24:5972–5980.

Cherry, R. J., and D. Chapman 1969. Optical properties of black lecithin films. *J. Mol. Biol.* 40:19–32.

den Engelsen, D., and B. de Koning. 1975. Ellipsometry of black lipid membranes of egg lecithin and chloroplast extracts. *Photochem. Photobiol.* 21:77–90.

Frehland, E., R. Kreikenbohn, and W. G. Pohl. 1982. Steady-state fluorescence polarization in planar lipid membranes. *Biophys. Chem.* 15:73–86.

Gianni, L., B. J. Corden, and C. E. Myers. 1984. The biochemical basis of anthracycline toxicity and antitumor activity. *Rev. Biochem. Tox.* 5:1–82.

Janiak, M. J., D. M. Small, and G. G. Shipley. 1976. Nature of the thermal pretransition of synthetic phospholipids: dimyristoyl- and dipalmitoyllecthin. *Biochemistry.* 15:4575–4580.

Janiak, M. J., D. M. Small, and G. G. Shipley. 1979. Temperature and compositional dependence of the structure of hydrated dimyristoyl lecithin. *J. Biol. Chem.* 254:6068–6078.

Jenkins, F. A., and H. E. White. 1957. Fundamentals of Optics. McGraw-Hill, New York.

Kawato, S., K. Kinosita, Jr., and A. Ikegami. 1977. Dynamic structure of lipid bilayers studies by nanosecond fluoresence techniques. *Biochemistry.* 16:2319.

Kinosita, K., Jr., and A. Ikegami. 1984. Reevaluation of the wobbling dynamics of diphenylhexatriene in phosphatidylcholine and cholesterol/phosphatidylcholine membranes. *Biochim. Biophys. Acta.* 769:523–527.

Kooyman, R. P. H., Y. K. Levine, and B. W. Van der Meer. 1981. Measurement of second and fourth rank order parameter by fluorescence polarization experiments in a lipid membrane system. *Chem. Phys.* 60:317–326.

Kooyman R. P. H., M. H. Vos, and Y. K. Levine. 1983. Determination of orientational order parameters in oriented lipid membrane systems by

---

[3]Corrections are applied to the data assuming the transition dipoles are parallel to the long axis of the fluorophore. Unfortunately, the orientation of some transition dipoles is not known. It is safe to assume that the dipoles are parallel to either the long or the short axis of the aromatic portion of the molecule. In absence of contradictory evidence, it is further assumed that the dipoles are parallel to the long axis.

angle-resolved fluorescence depolarization experiments. *Chem. Phys.* 81:461–472.

Lakowicz, J. R., and J. R. Knuston. 1980. Hindered depolarizing rotations of perylene in lipid bilayers. Detection by lifetime resolved fluorescence anisotropy measurements. *Biochemistry.* 19:905–911.

Lakowicz, J. R., F. G. Prendergast, and D. Hogen. 1979. Differential polarized phase fluorimetric investigations of diphenylhexatriene in lipid bilayers. Quantitation of hindered depolarizing rotations. *Biochemistry.* 18:508–519.

Mabrey, S., and J. M. Sturtevant. 1978. High-sensitivity differential scanning calorimetry in the study of biomembranes and related model systems. *Meth. Membr. Biol.* 9:237–274.

Murphee, S. A., D. Murphy, A. C. Sartorelli, and T. R. Tritton. 1982. Adriamycin-liposome interactions: a magnetic resonance study of the differential effects of cardiolipin on drug-induced fusion and permeability. *Biochim. Biophys. Acta.* 691:97–105.

Rogers, K. E., B. I. Carr, and Z. A. Tokes. 1983. Cell surface mediated cytotoxicity of polymer-bound adriamycin against drug-resistant hepatocytes. *Cancer Res.* 43:2741.

Stubbs, C. D., T. Kouyama, K. Kinosita, and A. Ikegami. 1981. Effect of double bonds on the dynamic properties of the hydrocarbon region of lecithin bilayers. *Biochemistry.* 20:4257–4262.

Szabo, A. 1980. Theory of polarized fluorescent emission in uniaxial liquid crystals. *J. Chem Phys.* 72:4620–4626.

Szabo, A. 1984. Theory of fluorescence depolarization in macromolecules and membranes. *J. Chem Phys.* 81:150–167.

Tritton, T. R., and J. A. Hickman. 1984. Cell surface membrane as a chemotherapeutic target. *In* Experimental and Clinical Progress in Cancer Chemotherapy. F. Muggia, editor. Martinus Nijoff, Boston, MA. 81–131.

Tritton, T. R., S. A. Murphree, and A. C. Sartorelli. 1978. Adriamycin: a proposal on the specificity of drug action. *Biochem. Biophys. Res. Commun.* 84:802–808.

Tritton, T. R., and G. Yee. 1982. The anticancer agent adriamycin can be actively cytotoxic without entering cells. *Science (Wash. DC).* 217:248–250.

Tritton, T. R., L. B. Wingard, and G. Yee. 1983. Immobilized adriamycin: a tool for separating cell surface from intracellular mechanisms. *Fed. Proc.* 42:284–287.

Tokes, Z. A., K. E. Rogers, and A. Rembaum. 1982. Synthesis of adriamycin-coupled polyglutaraldehyde microspheres and evaluation of their cytostatic activity. *Proc. Natl. Acad. Sci. USA.* 79:2026–2030.

Van der Meer B. W., R. P. H. Kooyman, and Y. K. Levine. 1982. A theory of fluorescence depolarization in macroscopically ordered membrane systems. *Chem. Phys.* 66:39–50.

Vos, M. H., R. P. H. Kooyman, and Y. K. Levine. 1983. Angle resolved fluorescence depolarization experiments on oriented lipid membrane systems. *Biochem. Biophys. Res. Commun.* 116:462–468.

Wigner, E. P. 1959. Group Theory and Its Application to the Quantum Mechanics of Atomic Spectra. Academic Press, Inc., New York.

Wingard, L. B., K. A. Eggler, and T. R. Tritton. 1984. Cell surface effects of adriamycin and carminomycin immobilized on cross-linked polyvinyl alcohol. *Cancer Res.* 45:3529–3536.

Yguerabide, J., and L. Stryer. 1971. Fluorescence spectroscopy of an oriented model membrane. *Proc. Natl. Acad. Sci. USA.* 68:1217–1221.

Yi, P. N., and R. C. MacDonald. 1973. Temperature dependence of optical properties of aqueous dispersions of phosphatidylcholine. *Chem. Phys. Lipids* 11:114–134.

Young, R. C., R. F. Ozols, and C. E. Myers. 1981. The anthracycline antineoplastic drugs. *New England J. Med.* 305:139–153.

Zannoni, C., A. Arcioni, and P. Cavatorta. 1983. Fluorescence depolarization in liquid crystals and membrane bilayers. *Chem. Phys. Lipids.* 32:179–250.